Case Report

Assessing the Impact of Geologic Contact Dilution in Ore/Waste Classification in the Gol-Gohar Iron Ore Mine, Southeastern Iran

Iman Masoumi [1] , **Gholamreza Kamali [1]**, **Omid Asghari [2],*** and **Xavier Emery [3],[4]**

[1] Department of Mining Engineering, Shahid Bahonar University of Kerman, Kerman 7616914111, Iran; imanmasoumi@eng.uk.ac.ir (I.M.); kamali@uk.ac.ir (G.K.)

[2] Simulation and Data Processing Laboratory, School of Mining Engineering, College of Engineering, University of Tehran, Tehran 1417414418, Iran

[3] Department of Mining Engineering, University of Chile, Santiago 8370448, Chile; xemery@ing.uchile.cl

[4] Advanced Mining Technology Center, University of Chile, Santiago 8370448, Chile

* Correspondence: o.asghari@ut.ac.ir; Tel.: +98-21-82084229

Abstract: Since the Gol-Gohar iron ore mine (GGIOM), which is located in southeastern Iran, is currently one of the biggest iron mines in this region, increasing the accuracy of its mineral resources model has become a challenge for geologists, metallurgists and mining engineers. Given that an accurate classification of the mining blocks into ore or waste is highly significant in strategic mine planning, three approaches for simulating the iron grades were compared against the true grades obtained from production data. The comparison was done by calculating the ratio between the total number of blocks correctly classified as ore and waste and the total number of misclassified blocks, and it was conducted for each approach in three mined benches at the GGIOM. The results reveal that the grade simulation that ignores the geological boundaries and the grade simulation based on a deterministic geological interpretation are much less accurate than the hierarchical approach, which consists of simulating both the geological boundaries and the grades.

Keywords: mining dilution; direct block simulation; truncated gaussian simulation; Gol-Gohar iron ore mine

1. Introduction

The proper classification of mineral resources and ore reserves, as well as an appropriate prediction of the amount of dilution and ore loss affect various mining activities, in particular, the development of geological and geometallurgical mineral resources models, the conversion of these resources into ore reserves, the definition of a production schedule, mine and plant designs, production management and grade control. The two interconnected phenomena of dilution and ore loss are caused by exploiting blocks (selective mining units) with different geological and metallurgical characteristics (lithology, alteration, mineralogy, in situ metal grade(s), recoverable grade(s), recovery ratio(s), etc.). Internal dilution, geologic contact dilution and operational mining dilution have been identified as the three primary sources of dilution that must be taken into account in evaluating mineral resources [1].

Predicting internal dilution and geologic contact dilution can also help decision-makers to assess and model uncertainty in long-term mine planning. So far, analytical, empirical, numerical, and analytical-empirical models have been mentioned in the literature on dilution assessment [2,3]. Most of these studies account for operating and operational parameters such as blast-hole pattern, type of equipment, as well as operational methods to evaluate the dilution. In this respect, Ebrahimi and Eng [4] proposed a geometrical model applicable to open pit mines and other investigations have

reviewed several previously introduced analytical-empirical models [5,6]. Moreover, Zarshenas and Saeedi [7] shed light on the impact of different types of risk (environmental, economic, and technical) on dilution for a group of mines in Iran, namely, the Sarcheshmeh open-pit mine, Gol-Gohar iron ore mine (GGIOM), and Moeil iron ore mine.

Internal dilution stems from the geological/geometallurgical characteristics of the mineralization and from predicting resources in a block volume distinct from that of the original data [8], which produces a decrease in the (in situ or recoverable) grade variability and a loss of selectivity due to the mixing of high and low grades within the block, known in geostatistics as the "support effect" [9]. It is worth noting that the support effect is a major issue in mineral resources modeling that occurs when the desirable volume for the final analysis is not equal to the initial volume of the sampling data. Geostatistical techniques such as nonlinear kriging [10,11] and direct block simulation (DBS) [12–14] were introduced to assess whether or not the average grade at the block support exceeds a cut-off grade and to classify the block as ore or waste, without the need to create a fine grid and to average the grade values predicted or simulated at the points of this grid [15,16]. This considerably reduces CPU time and memory requirements and make these techniques attractive for modeling large-scale deposits.

On the other hand, partitioning a deposit into domains on the basis of geological and geometallurgical interpretations is one of the main causes of uncertainty and can have a significant effect on prediction results such as dilution, ore loss, and mixture of populations. The most common uncertainty modeling approach in spatial grade distribution in a deposit begins by identifying the main geological and geometallurgical controls, such as lithology, alteration, mineralogy, weathering and faults, based on expert knowledge and available sampling data. The geological or geometallurgical domains can thus be delineated and the geostatistical prediction or simulation is ultimately achieved for each domain using its own available data [1,17].

The identification and modeling of domain boundaries plays a decisive role in grade prediction or simulation, as shown in several previous studies [18–20]. The assessment of mineral resources based on deterministic boundaries, whose output is only an interpretive layout at unsampled locations, often fails to accurately reflect stochastic changes in lithology and grade distributions [21,22]. To date, however, few authors have quantified the impact of boundary modeling on geologic contact dilution and ore/waste classification for long-term mine planning, which is the main objective and contribution of this work. Such modeling can be achieved through geostatistical simulations, which are used to construct multiple numerical realizations or outcomes of geological and geometallurgical domains. In addition to reproducing the spatial variability of the domain boundaries and to improving the quality of geological and geometallurgical interpretations, these outcomes contribute to measuring the uncertainty in the layout of domain boundaries. Several methods including sequential indicator simulation (SIS) [23,24], truncated Gaussian simulation (TGS) [25,26], plurigaussian simulation (PGS) [27,28] and multiple-point simulation (MPS) [29,30] are extensively employed in modeling domains. In particular, MPS, TGS, and PGS account for the contact relationships between domains and can enhance the reproduction of complex geometrical features [29–33].

The correct prediction of the dilution rate, and consequently, of the ore loss in each block—regardless of the amount of dilution or ore loss occurring during mining—requires the correct determination of its associated domain and grade, which can be achieved on the basis of exploration drill hole data. Similarly, accurate block classification can either reduce the uncertainty of long-term extraction plans or enhance production plans. The samples in the present study were taken from the GGIOM, which is located in southeastern Iran. It has reserves of more than 1.3 billion tons, making it one of the most important centers of iron ore production in Iran. All of the six deposits in this area are also in operation. In this respect, the detection of domain boundaries is a critical issue in these mines. Therefore, investigating an appropriate modeling approach for domain boundaries using drill hole and blast hole data is essential for the GGIOM.

Three different approaches for grade simulation and ore/waste classification were applied in extracted benches in this study to investigate internal dilution and geological contact dilution. These

approaches are: (1) DBS without lithological control, (2) deterministic boundary selection followed by DBS in each domain, and (3) hierarchical stochastic modeling of domains and grades. Then, the best approach was obtained through the introduction of coefficients of correct classification of ore and waste to incorrect classification of dilution and ore loss, thus comparing the simulated grades with the true grades of the mining blocks.

2. Materials and Methods

2.1. Principles of Geostatistical Simulation

In the modeling of all mineral deposits, quantitative variables are measured on continuous scales such as metal grades and categorical (nominal) variables such as rock types. While the exact values of these variables are known at a limited number of sampling locations, the goal is to determine these variables at unsampled locations.

Geostatistical simulation, which is used to construct resources and reserves models at different stages of a mining project, has become popular as a tool to reproduce the spatial variability of the original data. Various methods of simulation have been developed over the past decades [1,22,34]. Using stochastic simulation based on exploratory drill hole data also allows the assessment of different outcomes of the spatial distribution of continuous (grades) and categorical (lithology) variables. Therefore, it is possible to quantify uncertainty along with the spatial distribution of grades and domain boundaries. In this research, DBS was used to simulate grades and assess internal dilution, while TGS was implemented to simulate lithological domains.

2.2. Grade Simulation by DBS

Diamond core or reverse circulation drilling data represent a small volume in comparison with mining blocks (selective mining units). As a larger support is taken into account, high and low values tend to be averaged, which decreases the variability (measured, for instance, by the variance or the selectivity index) and generates a less skewed distribution. Internal dilution accounts for the variations in grade distribution as a function of the volume support, as fully investigated in [12,22,35]. In this study, the method proposed in [36] was used to simulate a continuous variable (in situ iron grade) on a block support, as per the following steps:

1. The drill hole grade data are transformed into normal scores.
2. A random path is defined to visit all the blocks targeted for simulation.
3. For each visited block:

- Normal values are simulated at a set of nodes discretizing the block, conditionally to available point- and block-support values (covariance functions and kriging systems are adapted in order to account for the different data supports);
- Each simulated normal value is back-transformed into a grade value;
- Grade values are averaged to obtain a block-support grade;
- Normal values are averaged to obtain a block-support normal value that is incorporated in the set of conditioning data for simulating the subsequent blocks;
- The block-support grade and normal value are preserved as the results, and the point-support values simulated at the discretizing nodes are removed.

The algorithm repeats the process of visiting each block following the random path until all the blocks are simulated.

2.3. Geological Domain Simulation by TGS

TGS simulates a Gaussian random field at all the target locations and then uses a truncation rule to transform the Gaussian values into geological domains. The main steps in TGS are as follows [27,37]:

Step 1. Two parameters controlling the simulation are inferred (i) thresholds that truncate the Gaussian random field into domains, which are determined based on the proportion of each domain, and (ii) the variogram model of the Gaussian random field, which is determined in order to reproduce the spatial relationship between the hard data.

Step 2. While the domains are known for each sample, their exact corresponding Gaussian values are unspecified; instead, only interval constraints are obtained. To break the deadlock, Gibbs sampling is used to generate Gaussian values conditionally to these interval constraints [27].

Step 3. The Gaussian random field is simulated at the target grid nodes, conditionally to the values obtained with Gibbs sampling. In this study, the turning bands algorithm is employed.

Step 4. In the last step, the truncation rule is used to convert the simulated Gaussian values at the grid nodes back into the geological domains.

2.4. Different Approaches for Block Classification

The simplest method for separating waste from ore is to plot their boundaries based on the lithological logs of exploration drill hole data. The complexity of geological structures also gives rise to lots of errors in manual classification. Another method for separating waste from ore is to resort to simple geological models. In this method, vertical and horizontal geological cross-sections are mapped, and then their combination is used to develop three-dimensional (3D) deposit models [38]. Employing only one geological interpretation also fails to determine uncertainties in the spatial configuration of domains, and consequently, fails to accurately differentiate waste, ore, dilution, and ore loss in each block.

In this paper, three different approaches were employed to establish geological boundaries based on geostatistical simulation, and their effects on the classification of ore blocks were subsequently studied:

Approach 1 (#APP1). A total of 100 DBS realizations of the iron grade were constructed without geological control.

Approach 2 (#APP2). Using a deterministic geological model based on lithological log data from drill holes, two domains were defined, consisting of all magnetite and magnetite-free rocks. Then, in each of these domains, 100 DBS iron grade realizations were constructed conditionally to the drill hole data.

Approach 3 (#APP3). A total of 100 realizations of the two domains were constructed by TGS. In each of these, the iron grade was simulated by DBS. Afterwards, 100-grade realizations were produced based on the 100 TGS outputs (a single grade realization is associated with each domain realization).

The last two approaches rely on a hierarchical modeling, where geological domains are first identified and grade is subsequently simulated in each domain based on DBS [22,39]. The two approaches differ in the way (deterministic or stochastic) they model the geological domains.

It should also be noted that geostatistical simulation yields one hundred block model realizations, and none of these realizations per se are assumed to be an appropriate prediction for the block in question.

2.5. Validation and Comparison of the Different Approaches

The results of the grade simulation obtained from the different approaches based on exploration drill hole data were compared with the actual grades calculated from the blast hole data, and the best approach for the classification of ore, waste, dilution, and ore loss was determined. Accordingly, the incorrect classifications of ore and waste as dilution and ore loss can be measured by comparing the simulated grades to those of the actual extraction grades of the mine in relation to a given cut-off grade. The output of this classification is presented in four groups (Figure 1):

- The block is simulated as ore and is extracted in the same class. In this case, there is no wrong classification (ore).
- The block is simulated as waste and extracted in the same class. In this case, there is no wrong classification (waste).

- The block is simulated as waste and extracted in the ore class based on the true grades of blast holes. In this case, the incorrect classification will cause the mix of ore in the waste dump (ore loss).
- The ore block is simulated as ore and extracted in the waste class based on the true grades of blast holes. In this case, the incorrect classification will lead to the entry of waste into the plant (dilution).
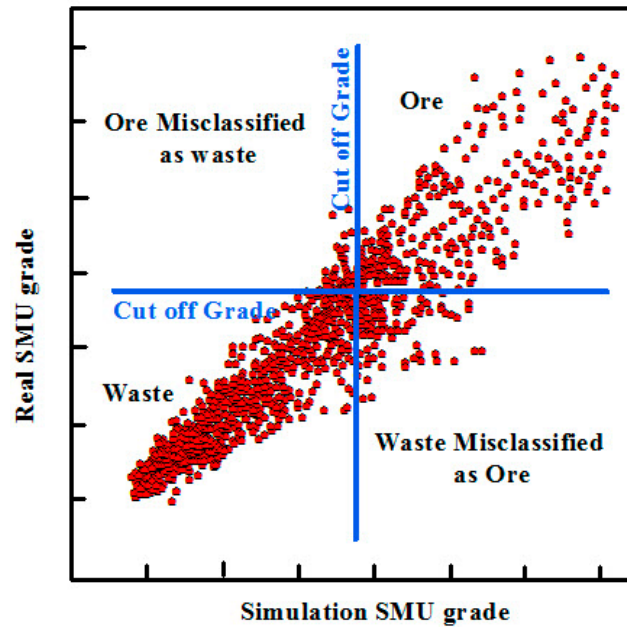

Figure 1. Two-dimensional (2D) graph of simulated grade vs. true grade.

In order to compare the results of the different approaches and to introduce the best approach, one code (between 1 and 4) was assigned to each block in each realization (Table 1). Then, using the confusion matrix, Figure 1 and Table 1 were developed for each of the 100 realizations in each approach, and the results were compared with the true grade values of the blocks. Figure 2 illustrates the classification matrix based on correct and incorrect results of a classification in each block. The sum of the values of diagonal components in Figure 2 is also equal to the correct classification states. In this study, the R-ratio value is equal to the sum of correct classifications of ore and waste blocks divided by the sum of incorrect classifications of dilution and ore loss ones. This ratio was calculated for each of the three approaches and each realization and its distribution over the 100 realizations is correspondingly evaluated. Equation (1) represents the proposed ratio for the final comparison of results in each approach. Here, assuming the same "cost'" for the different classes, the W1 to W4 coefficients are set to 1. Obviously, these coefficients can be corrected or changed in the case of extraction investigations in relation to cost functions and they can also be updated according to the conditions of each mine with regard to the correct and incorrect classification costs.

$$\text{R} = \frac{(W1)\times\text{Number of blocks classified as waste} +(W2)\times\text{Number of blocks classified as ore}}{(W3)\times\text{Number of blocks classified as dilution} +(W4)\times\text{Number of blocks classified as ore loss}} \qquad (1)$$

Table 1. Classification algorithm for each block in each simulation based on cut-off grade.

Code	Group	Blast-Hole Grade	Block Grade in Each Realization
1	Ore	>Cut-off grade	≥Cut-off grade
2	Waste	<Cut-off grade	≤Cut-off grade
3	Ore loss	>Cut-off grade	≤Cut-off grade
4	Dilution	<Cut-off grade	≥Cut-off grade

Simulation Results			
Waste	**Ore**		
Incorrect (Ore Loss)	Correct	Ore	True Grade
Correct	Incorrect (Dilution)	Waste	

Figure 2. Formation of classification matrix based on true and simulated grades.

Figure 3 provides the algorithm of operations used to determine the best approach to select geological boundaries for proper classification and correct prediction of dilution and ore loss in each block used in the GGIOM.
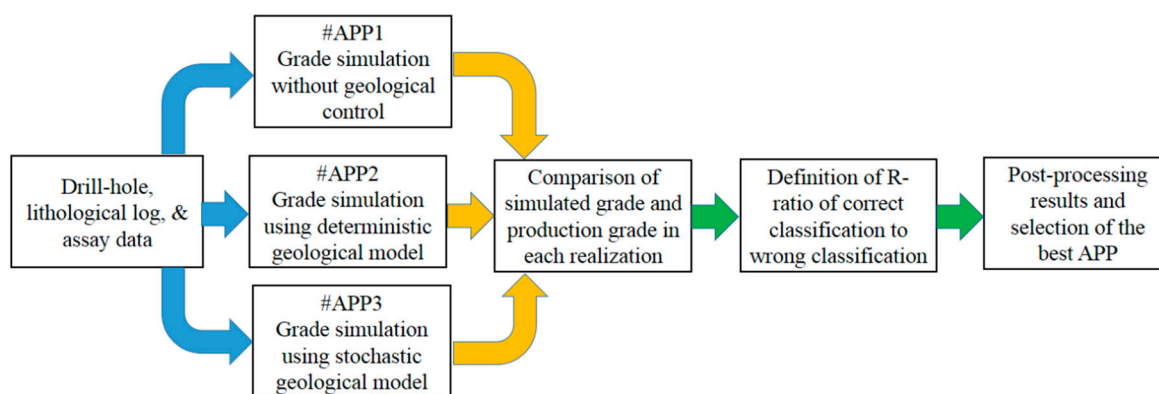

Figure 3. Algorithm for selection of the best approach based on results of block classifications.

3. Case Study

3.1. Geological Description and Problem Statement

The Gol-Gohar iron ore deposit is located at about 55 km southwest of Sirjan on the eastern edge of the Sanandaj-Sirjan structural zone of Iran. Figure 4 shows a geological map of the study area. This deposit is also hosted in metamorphosed sedimentary and volcanic rocks of greenschist facies [40]. As evidenced by drill hole cores, the main lithology types around this deposit are quaternary sediments, conglomerate, limestone, dolomite, gneiss, amphibolite, and mica schist.

The deposit is mined by open pit and the length of the deposit is about 1 km from north to south and 2 km east to west. In each bench, mined materials are classified into ore and waste based on their economic value. The extraction operations in this mine are planned in accordance to specified geological polygons, drawn at different height levels based on the lithology of drill hole cores. Since the average distance between drill holes is approximately 50 to 100 m and the arrangement of geological boundaries is complex, the uncertainty in the geological boundaries in mapped sections is high.

It should be noted that in short-term mine planning, increasing the financial return is normally done by rectifying the geological boundaries based on blast hole data and grade control during mine extraction. Generally, the classification of ore and waste is performed based on the blast hole data. In long-term mine planning wherein production data is not available, the main concern is the prediction of geological boundaries based on drill hole data, which provide less information on the geology and grades. Accordingly, we need to compare several approaches that delineate the geological domains in order to find a methodology that improves the final block classification.
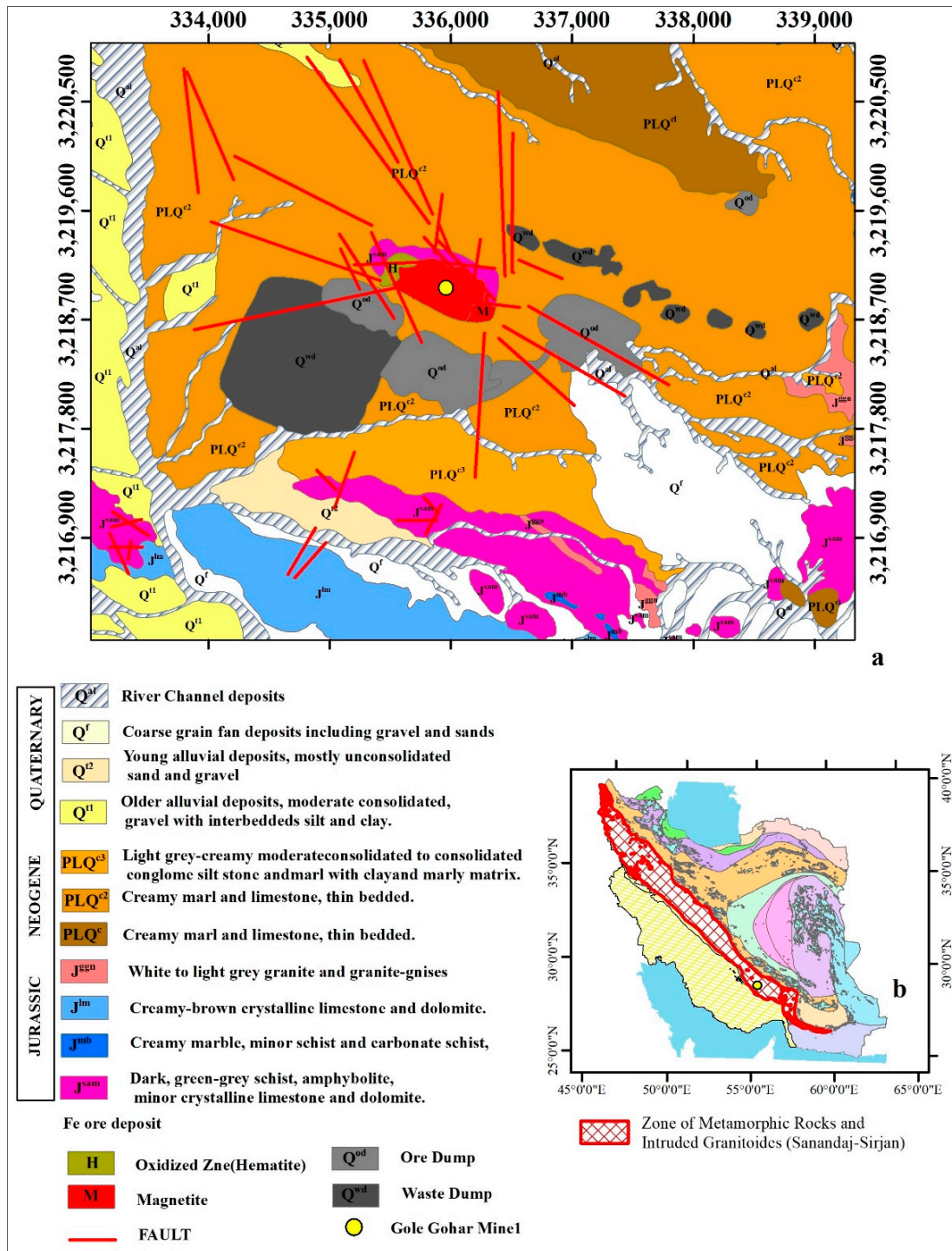
Figure 4. (**a**) Geological map of Gol-Gohar iron ore deposit, scale 1:25,000, (**b**) Location of Gol-Gohar iron ore deposit in the Sanandaj-Sirjan structural zone.

3.2. Data Presentation

The study area is composed of two main rock domains. The first domain is a set of schist, amphibolite, and gneiss with no magnetite mineralization, with in situ iron grades of less than 10%. The second domain includes rocks containing magnetite mineralization. A statistical summary of the drill hole data for both rock domains and their histograms are presented in Table 2 and Figure 5. In the first part of the second domain, the dispersion of magnetite in schist rock signifies iron ore

grades between 19% and 25%. The last part of this domain contains higher iron grades, which is clearly evident in fully magnetized rocks. Figure 6 shows the drilling cores depending on the lithology. High magnetite iron ore and interbedded magnetite in crushed schist, most commonly referred to as iron ore alteration in the mine, are illustrated in Figure 6a,c,d, respectively. Notably, it is very difficult to distinguish schist layers between magnetite. Also, cores from amphibolite and gneiss are shown in Figure 6b.

Table 2. Statistical data of in situ iron grade (%) in the overall deposit and for each rock type domain.

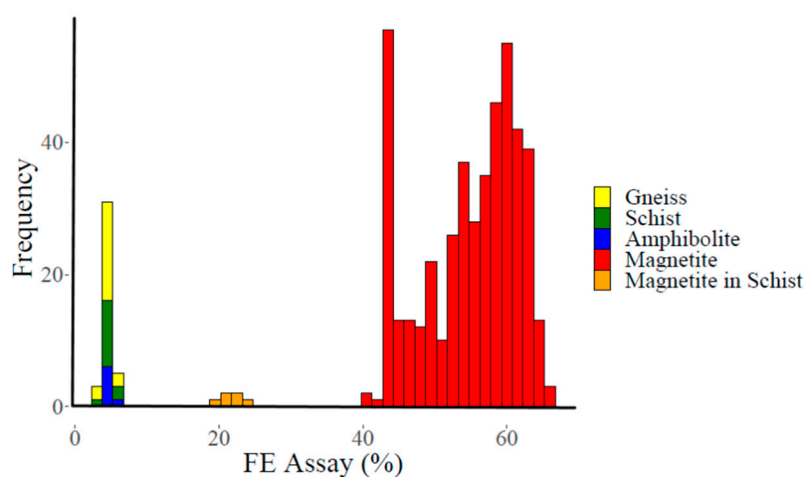| Domains	Lithology Type	Number of Data	Mean	Median	Standard Deviation	Variance	Minimum	Maximum
A	Amphibolite	7	5.07	5.1	0.518	0.269	4.5	6.1
	Gneiss	19	4.72	4.8	0.694	0.482	3.4	6.5
	Schist	13	4.815	4.9	0.767	0.590	3.20	6.1
B	Magnetite	454	54.89	56.55	6.698	44.86	39.9	66.2
	Magnetite in schist	6	21.96	22.050	1.678	2.819	19.2	24.4
	Total	499	50.58	55.20	15.22	231.69	3.20	66.2

Figure 5. Histogram of raw data for global lithology types.

Figure 6. Different types of lithology in the Gol-Gohar iron ore mine (GGIOM). (**a**) High-grade magnetite, (**b**) amphibolite, (**c**) gneiss, and (**d**) magnetite in schist.

As indicated in the histogram of the grade data, the first domain has a narrower grade variation than the magnetite-containing rock domain. On the other hand, the rock types in the first domain

lack economically viable mineralization and are also associated with waste blocks that should not be transferred to the plants. Therefore, geologists need to select the most appropriate approach for predicting the contact between these two types of lithology.

Figure 7 displays a contact analysis for the given domains, which consists of plotting the average iron grade in each domain as a function of the signed distance to the other domain [1]. This analysis indicates a hard boundary between contained and non-contained magnetite domains, insofar as the mean iron grade is discontinuous when crossing the boundary. Accordingly, a hierarchical modeling (Approaches 2 and 3) is expected to outperform the modeling that ignores the geological control (Approach 1).
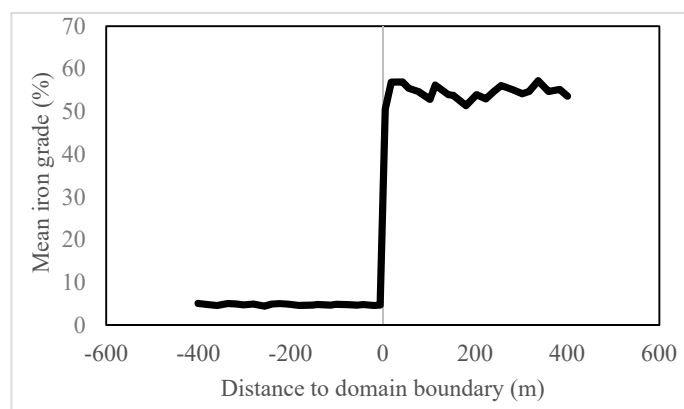
Figure 7. Mean values of in situ iron grade as a function of the signed distance to the domain boundary.

Figure 8a shows a 3D dispersion of the iron grades measured in the exploration drill hole cores and Figure 8b illustrates the grades in three extraction benches determined by blast hole data. The low-grade samples (blue points in Figure 8a,b) appear to be scattered in between the high-grade samples, suggesting that domains A and B are spatially intermingled, with a complex geometry of their boundaries.
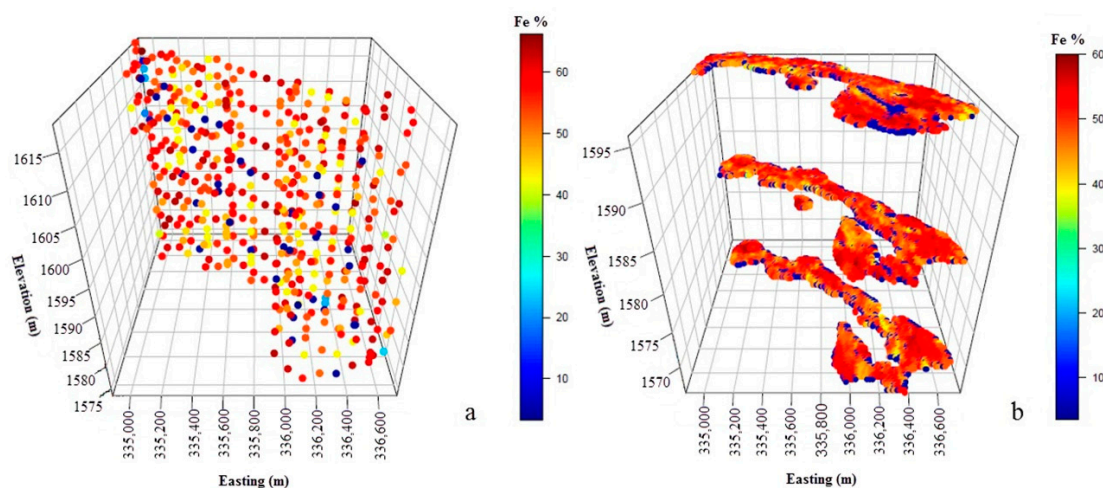

Figure 8. (**a**) Location map of grade measured at drill hole data. (**b**) Blast hole assay data in three benches. Colors indicate the in situ iron grade.

Table 3 summarizes the statistical parameters of the drill hole grades and blast hole grades in the three exploitation benches at GGIOM.

Table 3. Basic statistics of iron grades in drill-holes and blast-holes.

Type of Data	Parameter	Number of Data	Lower Quartile	Upper Quartile	Minimum	Maximum	Mean	Variance	Coefficient of Variation
Drill hole	Iron (%)	499	46.6	60.1	3.2	66.2	50.58	231	0.301
Blast hole	Iron (%)	10998	46.8	53.52	3.5	59.16	46.45	185.97	0.294

Ordinary kriging with blocks of 10 m × 10 m × 15 m was applied to calculate the block grades based on 10,998 blast holes, which are on a fine sampling mesh with an average distance of 5 m apart and a depth of 15 m drilled in the exploitation benches. Due to the very dense network of blast holes, the kriging error is negligible and can be ignored, hence the kriged grade can be considered as the true grade against which the simulated grades based on drill-hole information will be compared.

3.3. Stochastic Modeling of Rock Type Domains

Truncated Gaussian simulation (TGS) allows modeling of the two geological domains (A and B, Table 2) through the truncation of a Gaussian random field (Y, upper case) at a specific threshold y (lower case):

- Location x belongs to domain A $\leftrightarrow Y(x) < y$
- Location x belongs to domain B $\leftrightarrow Y(x) > y$

The threshold y was set to −1.419 in order to reflect the global proportion of domain A and B (7.8% and 92.2%, respectively). Table 4 outlines the specifications of the Gaussian variogram model, whose main directions of anisotropy are aligned with the coordinate axes.

Table 4. Specifications of the Gaussian variogram model in truncated Gaussian simulation (TGS).

Model Type	Range (m)			Direction 1		Direction 2		Direction 3	
	R1	R2	R3	Dip	Az	Dip	Az	Dip	Az
Spherical	195	85	4.5	0	0	0	90	90	0

3.4. Results

To investigate the proposed methods for block classification, the scatterplot of the simulated grade vs. the true grade is drawn for each realization according to Table 1. Figure 9 shows the scatterplots of the 50th and the 100th realizations for the three approaches. Considering an economic cut-off grade of 20% to separate ore and waste, four different classes are specified in these charts. As shown in the diagram of Approach 1, none of the blocks are in the waste group and very few (1 or 2 blocks) are in the ore loss group, which can be explained because the grades are conditioned to many high- and few low-grade data, therefore this tends to deliver a simulated grade that is higher than the cut-off. A large number of waste blocks were misclassified as ore (dilution group) that could be mined. The classification improves with Approaches 2 and 3, which account for the geological control.

Figure 10 shows the average of the iron grade over the 100 realizations for each approach, as well as the true grades in four categories with various colors. The average results from Approach 2 agree with reality only in the waste lens of the eastern part of the first bench; elsewhere, the average simulated grade does not show good agreement with the true grade, most likely due to poor delineation of the geological domains based on the drill hole information. The visual comparison with the average grade obtained in Approach 3 suggests higher compliance compared with the other two approaches, due to more realistic modeling of the geological domains and of the uncertainty in their boundaries.
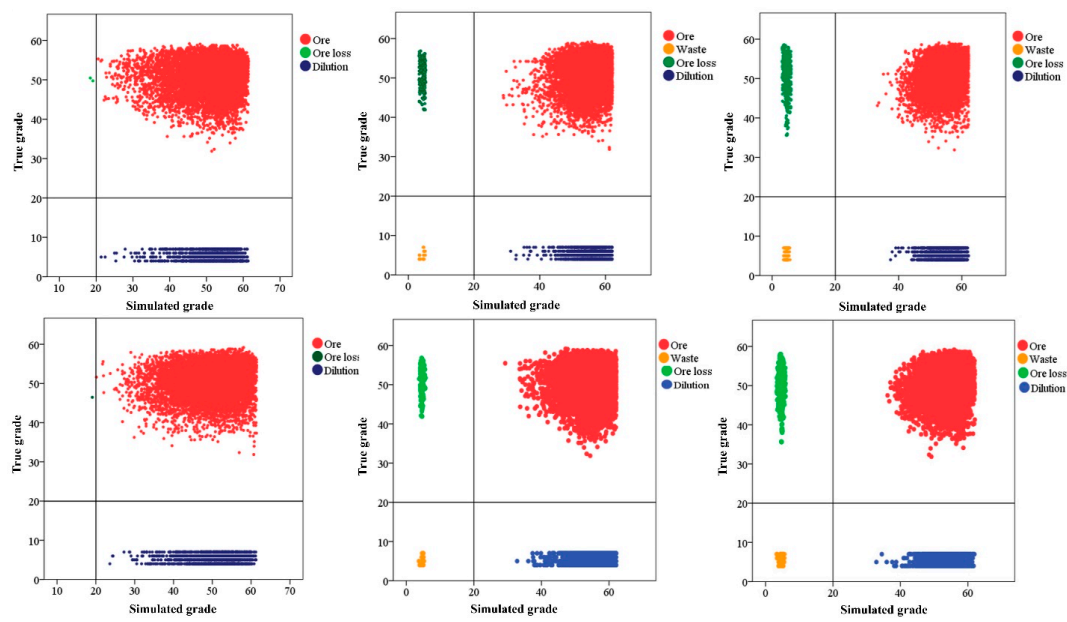
Figure 9. Scatterplots of simulated grades vs. real grades for two realizations and three approaches. Left: Approach 1; center: Approach 2; right: Approach 3. Top: realization 50; bottom: realization 100.
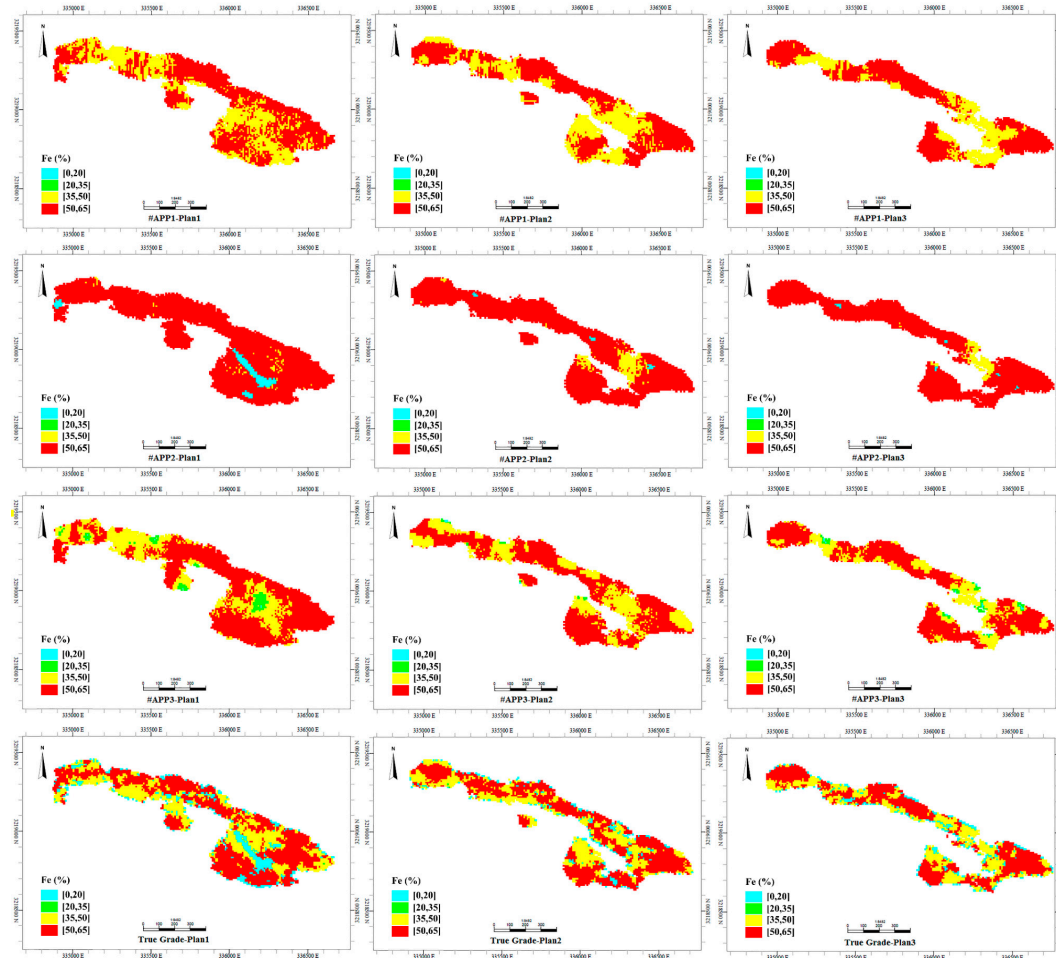
Figure 10. Average simulated grade over 100 realizations obtained with each approach for three extraction benches vs. true grade of the same benches. From top to bottom: Approach 1, Approach 2, Approach 3 and reality.

Based on the simulated information, the R-ratio of the number of blocks correctly classified as ore or waste with the number of wrongly classified blocks (dilution and ore loss) was calculated for each realization based on Equation (1). The distribution of this ratio for different cut-off grades ranging from 15% to 40% is presented in Figure 11 for the three discussed approaches. According to these charts, the block classification with Approach 3 is consistently better than with the other two approaches, suggesting a better modeling of the geological variability, while Approach 1 leads to the lowest ratios for all the cut-off grades.
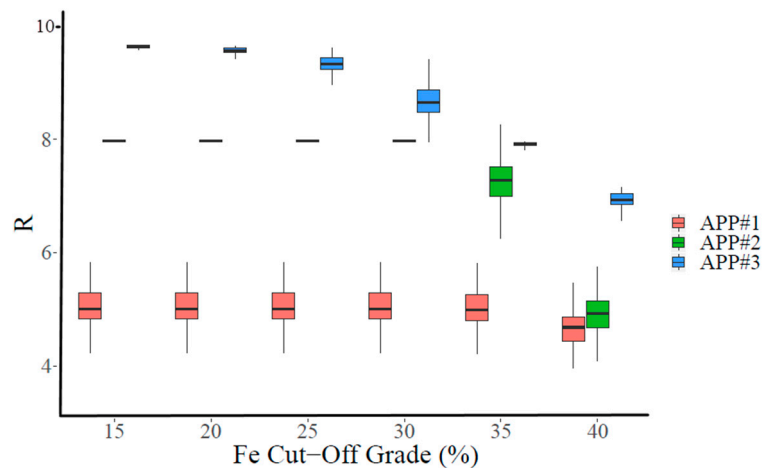
Figure 11. Box plots of distribution of the R-ratio for three approaches and cut-off grades between 15% and 40%.

In addition, the results of each approach were compared based on the mean error percentage (MEP) for each of the 100 realizations, according to Equation (2) [41]:

$$MEP(K) = \frac{1}{n_{blocks}} \sum_{i=1}^{n_{blocks}} 100 \times \frac{S^K(i) - R(i)}{R(i)} \qquad (2)$$

where $S^K(i)$ is the simulated grade for block i, $R(i)$ is the true block grade, and n_{blocks} represents the number of simulated blocks. The error distribution is significantly less dispersed around zero with Approach 3 and more dispersed with Approach 1, which confirms that the former is more accurate than the latter when predicting the iron grades (Figure 12).
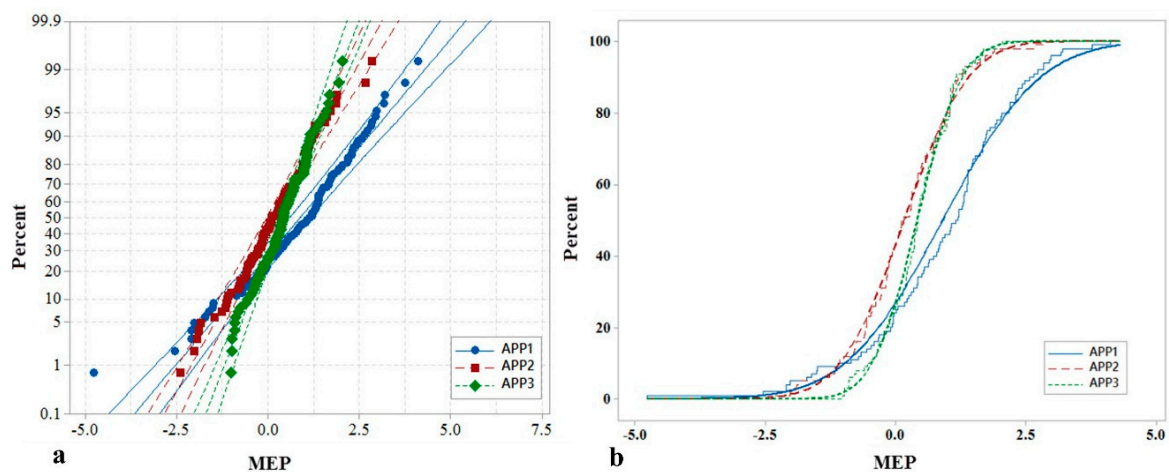

Figure 12. Cumulative distribution function (**a**) and probability plot (**b**) of the mean error percentage (MEP) calculated over 100 realizations.

4. Conclusions

Classifying waste and ore blocks is of utmost importance for geological/geometallurgical modeling of mineral resources, long-term planning and mine/plant design in the GGIOM. Given the complexity of the geometry of rock types containing magnetite and without it, the block models constructed solely on the basis of grade information and that ignore lithological controls, provide poor ore/waste classification in comparison with the hierarchical approaches that model the geometry of the rock type domains first, and then the iron grades within each domain.

An interpretation of domain boundaries based on drill hole data and empirical knowledge is an indispensable method for understanding the type of ore deposit, developing geological and geometallurgical models, as well as for extraction design and mineral processing studies. However, this logical approach fails to reproduce the variability in real domain boundaries and does not incorporate the uncertainty in the boundary layout insofar as it relies on a single deterministic model. As a consequence, this approach creates a significant error in production models, which results in significant errors in grade and ore/waste classification models. With regard to the GGIOM, it is critical to account for the lithological boundary variability and uncertainty in order to determine the final destination of each block in the long-term.

This study advocates for stochastic modeling of both lithological boundaries and grades, which consists of simulating the lithological domains that control the mineralization before simulating the metal grade in each domain, under the premise that the domain boundaries are associated with a clear-cut discontinuity of the grades ("hard" boundaries). The superiority of this approach is corroborated by comparing the simulated grades with the true grades derived from the blast hole information, and it is quantified by the ratio between the correct and incorrect ore/waste classifications of the mining blocks for different cut-off grades. Fewer classification errors have an impact on the predicted ore tonnages and all of the future mining plans.

References

1. Rossi, M.E.; Deutsch, C.V. *Mineral Resource Estimation*; Springer Science & Business Media: Dordrecht, The Netherlands, 2013.
2. Popov, G.N. *The Working of Mineral Deposits*; Mir Publishers: Moscow, Russia, 1971.
3. Saeedi, G.; Shahriar, K.; Rezai, B.; Karpuz, C.E.L.A.L. Numerical modelling of out-of-seam dilution in longwall retreat mining. *Int. J. Rock Mech. Min. Sci.* **2010**, *47*, 533–543. [CrossRef]
4. Ebrahimi, A.; Eng, P. The importance of dilution factor for open pit mining projects. In Proceedings of the 23rd World Mining Congress, Montreal, QC, Canada, 11–15 August 2013.
5. Yihong, L.; Weijin, Z. Reducing waste-rock dilution in narrow-vein conditions at tungsten mines in China. *Min. Sci. Technol.* **1986**, *4*, 1–7. [CrossRef]
6. Mubita, D. Recent initiatives in reducing dilution at KonKola Mine, Zambia. *J. South. Afr. Inst. Min. Metall.* **2005**, *105*, 107–112.
7. Zarshenas, Y.; Saeedi, G. Risk assessment of dilution in open pit mines. *Arab. J. Geosci.* **2016**, *9*, 209. [CrossRef]
8. Parker, H. The volume variance relationship: A useful tool for mine planning. *Eng. Min. J.* **1979**, *180*, 106–123.

9. Matheron, G. The selectivity of the distributions and the 'second principle of geostatistics'. In *Geostatistics for Natural Resources Characterization*; Springer: Dordrecht, The Netherlands, 1984; pp. 421–433.

10. Rivoirard, J. *Introduction to Disjunctive Kriging and Non-Linear Geostatistics*; Oxford University Press: Oxford, UK, 1994.

11. Hekmatnejad, A.; Emery, X.; Alipour-Shahsavari, M. Comparing linear and non-linear kriging for grade prediction and ore-waste classification in mineral deposits. *Int. J. Min. Reclam. Environ.* **2019**, *33*, 247–264. [CrossRef]

12. Journel, A.G.; Huijbregts, C.J. *Mining Geostatistics*; Academic Press: London, UK, 1978.

13. Godoy, M. The Effective Management of Geological Risk in Long-Term Scheduling of Open Pit Mines. Ph.D. Thesis, University of Queensland, Brisbane, Australia, 2003.

14. Benndorf, J.; Dimitrakopoulos, R. New Efficient Methods for Conditional Simulations of Large Orebodies. In *Advances in Applied Strategic Mine Planning*; Springer: Berlin/Heidelberg, Germnay, 2018; pp. 353–369.

15. Verly, G. The block distribution given a point multivariate normal distribution. In *Geostatistics for Natural Resources Characterization*; Springer: Berlin/Heidelberg, Germany, 1984; pp. 495–515.

16. Journel, A.G.; Kyriakidis, P.C. *Evaluation of Mineral Reserves: A Simulation Approach*; Oxford University Press: Oxford, UK, 2004.

17. Duke, J.; Hanna, P. Geological interpretation for resource modelling and estimation. In *Mineral Resource and Ore Reserve Estimation—The AusIMM Guide to Good Practice*; The Australasian Institute of Mining and Metallurgy: Carlton, Australia, 2001; pp. 147–156.

18. Ortiz, J.M.; Emery, X. Geostatistical estimation of mineral resources with soft geological boundaries: A comparative study. *J. S. Afr. Inst. Min. Metall.* **2006**, *106*, 577–584.

19. Maleki, M.; Emery, X. Joint simulation of stationary grade and non-stationary rock type for quantifying geological uncertainty in a copper deposit. *Comput. Geosci.* **2017**, *109*, 258–267. [CrossRef]

20. Emery, X.; Maleki, M. Geostatistics in the presence of geological boundaries: Application to mineral resources modeling. *Ore Geol. Rev.* **2019**, *114*, 103124. [CrossRef]

21. Journel, A. The deterministic side of geostatistics. *J. Int. Assoc. Math. Geol.* **1985**, *17*, 1–15. [CrossRef]

22. Chilès, J.-P.; Delfiner, P. *Geostatistics: Modeling Spatial Uncertainty*; John Wiley & Sons: Hoboken, NJ, USA, 2012.

23. Journel, A.G.; Alabert, F.G. New method for reservoir mapping. *J. Pet. Technol.* **1990**, *42*, 212–218. [CrossRef]

24. Isaaks, E.H. The Application of Monte Carlo Methods to the Analysis of Spatially Correlated Data. Ph.D. Thesis, Stanford University, Stanford, CA, USA, 1990.

25. Galli, A.; Beucher, H.; le Loc'h, G.; Doligez, B.; Group, H. The pros and cons of the truncated Gaussian method. In *Geostatistical Simulations*; Springer: Berlin/Heidelberg, Germany, 1994; pp. 217–233.

26. Skvortsova, T.; Armstrong, M.; Beucher, H.; Forkes, J.; Thwaites, A.; Turner, R. Simulating the geometry of a granite-hosted uranium orebody. In *Geostatistics Rio 2000*; Springer: Berlin/Heidelberg, Germany, 2002; pp. 85–99.

27. Armstrong, M.; Galli, A.; Beucher, H.; le Loc'h, G.; Renard, D.; Doligez, B.; Eschard, R.; Geffroy, F. *Plurigaussian Simulations in Geosciences*; Springer Science & Business Media: Berlin, Germany, 2011.

28. Le Loc'h, G.; Beucher, H.; Galli, A.; Doligez, B. Improvement in the truncated Gaussian method: Combining several Gaussian functions. In *Ecmor iv-4th European Conference on the Mathematics of Oil Recovery*; European Association of Geoscientists & Engineers: DB Houten, The Netherlands, 1994.

29. Strebelle, S. Conditional simulation of complex geological structures using multiple-point statistics. *Math. Geol.* **2002**, *34*, 1–21. [CrossRef]

30. Mariethoz, G.; Caers, J. *Multiple-Point Geostatistics: Stochastic Modeling with Training Images*; John Wiley & Sons: Hoboken, NJ, USA, 2014.

31. Talebi, H.; Sabeti, E.H.; Azadi, M.; Emery, X. Risk quantification with combined use of lithological and grade simulations: Application to a porphyry copper deposit. *Ore Geol. Rev.* **2016**, *75*, 42–51. [CrossRef]

32. Madani, N.; Emery, X. Simulation of geo-domains accounting for chronology and contact relationships: Application to the Río Blanco copper deposit. *Stoch. Environ. Res. Risk Assess.* **2015**, *29*, 2173–2191. [CrossRef]

33. Mery, N.; Emery, X.; Cáceres, A.; Ribeiro, D.; Cunha, E. Geostatistical modeling of the geological uncertainty in an iron ore deposit. *Ore Geol. Rev.* **2017**, *88*, 336–351. [CrossRef]

34. Emery, X.; Gonzalez, K.E. Incorporating the uncertainty in geological boundaries into mineral resources evaluation. *J. Geol. Soc. India* **2007**, *69*, 29.

35.   Isaaks, E.H.; Srivastava, R.M. *An introduction to Applied Geostatistics*; Oxford University Press: Oxford, UK, 1989.

36.   Benndorf, J.; Dimitrakopoulos, R. New efficient methods for conditional simulation of large orebodies. In *Orebody and Strategic Mine Planning*; The Australasian Institute of Mining and Metallurgy: Carlton, Australia, 2007; pp. 103–110.

37.   Cáceres, A.; Emery, X.; Riquelme, R. Truncated Gaussian kriging as an alternative to indicator kriging. In *Proceedings of 4th International Conference on Mining Innovation*; Gecamin Ltda: Santiago, Chile, 2010; pp. 367–376.

38.   Sides, E. Geological modelling of mineral deposits for prediction in mining. *Geol. Rundsch.* **1997**, *86*, 342–353. [CrossRef]

39.   Roldão, D.; Ribeiro, D.; Cunha, E.; Noronha, R.; Madsen, A.; Masetti, L. Combined use of lithological and grade simulations for risk analysis in iron ore, Brazil. In *Geostatistics Oslo 2012*; Springer: Berlin/Heidelberg, Germany, 2012; pp. 423–434.

40.   Babaki, A.; Aftabi, A. Investigation on the model of iron mineralization at Gol Gohar iron deposit, Sirjan-Kerman. *Geosci. Sci. Q. J.* **2006**, *61*, 40–59.

41.   Cáceres, A.; Emery, X. Conditional co-simulation of copper grades and lithofacies in the Río Blanco–Los Bronces copper deposit. In *Proceedings of the 4th International Conference on Mining Innovation*; Gecamin Ltda: Santiago, Chile, 2010; pp. 311–320.